

# Effects of Anti-VEGF Treatment on the Recovery of the Developing Retina Following Oxygen-Induced Retinopathy

Clayton C. Tokunaga, Kenneth P. Mitton, Wendelin Dailey, Charlotte Massoll, Kevin Roumayah, Ed Guzman, Noor Tarabishy, Mei Cheng, and Kimberly A. Drenser

Pediatric Retinal Research Laboratory, Eye Research Institute, Oakland University, Rochester, Michigan

Correspondence: Kimberly A. Drenser, Pediatric Retinal Research Laboratory, Eye Research Institute, Oakland University, 2200 North Squirrel Road, Rochester, MI 48309-4401; kdrenser@arcpc.net.

Kenneth P. Mitton, Eye Research Institute, Oakland University, Room 412 Dodge Hall, Rochester, MI 48309; mitton@oakland.edu.

Submitted: October 7, 2013

Accepted: February 1, 2014

Citation: Tokunaga CC, Mitton KP, Dailey W, et al. Effects of anti-VEGF treatment on the recovery of the developing retina following oxygen-induced retinopathy. *Invest Ophthalmol Vis Sci.* 2014;55:1884-1892. DOI:10.1167/iovs.13-13397

**PURPOSE.** Inhibition of VEGF is widely used in patients to control neovascularization and decrease vascular permeability. To date, the effect of VEGF inhibition has not been evaluated in the developing retina such as that seen in premature infants. The goal of this study was to address the effect of anti-VEGF treatment on retinal development of a mouse model of retinopathy.

**METHODS.** C57BL/6J mice were evaluated using a model of oxygen-induced retinopathy. Test animals were treated at postnatal day (P) 14 with intravitreal injections of the VEGF inhibitor aflibercept (2.5 or 10  $\mu$ g) in one eye. Control animals were treated with injection of PBS in one eye. The noninjected fellow eyes were used as internal controls. Areas of avascular retina and neovascular tufts in injected (treated) eyes and noninjected fellow eyes were determined at P17, and the difference related to these characteristics was obtained among them. To evaluate the effect of VEGF inhibition on neurogenesis, focal ERG was performed at P21 and P42. Histologic evaluation of the retinal structure was also evaluated at P42.

**RESULTS.** Aflibercept treatment reduced the amount of neovascular tufts but significantly increased the area of avascular retina (low dose and high dose) at P17. The delayed vascular growth corresponded to decreased ERG amplitudes (at P21 and P42) and structural changes in the retinal layers that persisted (at P42), despite vascular recovery.

**CONCLUSIONS.** Inhibition of VEGF in developing eyes has the short-term effect of delayed vascular growth and the long-term effects of decreased function with persistent changes in the neuroretinal structures.

**Keywords:** retinopathy of prematurity, neurovascular niche, VEGF, anti-VEGF, aflibercept

A aberrant vascular structure in the eye is associated with a wide variety of diseases, including congenital, hereditary, and acquired disorders. Problems with vasculature in the retina may be associated with incomplete vascular development or pathologic responses to injury. Areas of hypoxic or ischemic retina alter the normal biochemical balance that regulates both vascular growth and neural growth, resulting in pathologic changes. Several primary molecules regulating vascular growth also direct neural growth.<sup>1,2</sup> Therefore, it is not surprising that areas of retina that are devoid of normal vasculature also have decreased function. An example of this phenomenon is seen in the premature retina. Premature infants are born prior to completion of vascular networks in the periphery of the retina. Retinopathy of prematurity (ROP) progressing to prethreshold type 1 disease will require intervention with ablation of the peripheral avascular retina in order to destroy ischemic tissue and reduce metabolic demand. Investigations have shown that even with successful intervention and grossly normal structure the visual function is diminished.<sup>3,4</sup>

In the past, decreased function was attributed to the ablation treatment itself and unseen microscopic structural changes. However, it is more likely that the delayed vascular development and/or vaso-obliteration in the premature infant slows and even inhibits normal neurogenesis. Biochemical

changes in the avascular retina result in increased levels of semaphorin 3A, which inhibits neural cone growth and angiogenesis by competing for VEGF binding.<sup>5</sup> The unintended effect is the inhibition of appropriate VEGF-mediated growth.<sup>5</sup> Concomitantly, the oxygen-starved tissues cause VEGF expression to increase to abnormally high levels, which results in pathologic vascular changes in healthy, vascularized tissues.<sup>6</sup> This series of biochemical events places the premature infant at risk for permanent decreased visual function due to the delay (up to 3 months) in retinal vascularization. VEGF has a critical role in endothelial cell proliferation and morphogenesis. Overexpression of VEGF results in dysregulation of endothelial cell orientation.<sup>7</sup> Blocking VEGF action, therefore, seems logical in order to prevent the pathologic vascular changes that occur in ROP. However, nonvascular cells (e.g., Müller cells) express VEGF receptors and have a role in neurogenesis.<sup>8</sup> With the current use of VEGF-blocking pharmacological agents for the treatment of ROP, it is imperative to understand and define the interdependent roles of angiogenesis and neurogenesis. Angiogenesis as it relates to retinal disease is far better understood and therefore the primary outcome measurement in this study. Neurogenesis is less understood and as it relates to neurovascular development is looked at in relation to vascular growth and recovery.

VEGF is a proangiogenic factor that has been identified as a key player in a number of retinal diseases such as choroidal neovascular complexes, AMD, retinal vascular occlusion, diabetic retinopathy, ROP, and other inherited vitreoretinopathies.<sup>9</sup> In the healthy retina, intraretinal VEGF promotes and directs capillary bed growth and vascular remodeling. In diseased states, VEGF becomes elevated and promotes pathologic vascularization, leading to uncontrolled growth of endothelial buds. Vascular tight junctions are also regulated by VEGF,<sup>10</sup> whereby excessive VEGF leads to breakdown of the blood-retina barrier from permeable vascular walls.<sup>11,12</sup> Interestingly, VEGF also has a role in promoting neuroprotection and neurogenesis, thus highlighting the overlap between angiogenesis and neurogenesis.<sup>13</sup> Excessive VEGF leads to unwanted vascular growth, bleeding, and exudation, but complete loss of VEGF promotes loss of capillaries and atrophic changes to the neural retina. To date, VEGF blockade is administered in a “one size fits all” manner, with no distinction between the degree of pathology or assessment of VEGF levels. Herein, we present data investigating the short-term and long-term effects of VEGF blockade by aflibercept (a VEGF receptor decoy) on neurovascular recovery and maturation in a model of retinopathy.

## METHODS

All animal care and tissue collections performed in this study were carried out with the approval of Oakland University's Animal Care and Use Committee and conformed to the US Department of Agriculture standards and the ARVO Statement for the Use of Animals in Ophthalmic and Vision Research. C57BL/6J mice were obtained from Charles River Laboratories (Wilmington, MA). Mice were housed at Oakland University in a facility approved by the Association for Assessment and Accreditation of Laboratory Animal Care International.

### Mouse Model

An oxygen-induced retinopathy (OIR) model using C57BL/6J mice neonates was used in this study as previously described.<sup>14</sup> Briefly, at postnatal day (P) 7, mice were exposed to 75% oxygen for 5 consecutive days. At P12, mice were removed from the oxygen chamber and returned to room air (RA). They were divided into two treatment groups and two control groups. All pups were weighed at birth, treatment, and euthanasia to ensure that pups of similar weight were used in each group at each time point. Using a 34-gauge beveled needle (NanoFil; World Precision Instruments, Sarasota, FL), mice in the treatment groups received an intravitreal injection of 1  $\mu$ L aflibercept (Eylea; Regeneron Pharmaceutical, Tarrytown, NY) in the right eye at P14. Aflibercept is dissolved in an isotonic liquid (10 mM sodium phosphate, 40 mM sodium chloride, 0.03% polysorbate 20, and 5% sucrose [pH 6.2]). Two doses were tested (2.5 and 10  $\mu$ g diluted in sterile PBS) in order to evaluate possible differences with dosing regimens. Dosing equivalent to that used in humans (10  $\mu$ g) was estimated based upon relative vitreal volumes. Because each litter might have a different level of OIR depending on the weight<sup>15</sup> (despite all animals being killed at the same time point), the fellow eye was not injected, being left as an internal control. Because a fellow eye effect is often noted following intravitreal treatments of one eye, mice in one of the control groups underwent intravitreal injection of 1  $\mu$ L PBS in the right eye, and the other eye remained untreated. This also controls for the effect of injection alone. Last, animals in another control group did not receive any injections. Mice killed at P15 and P17 were used to evaluate retinal vascularization, and other animals

killed at P21 and P42 were used to assess retinal function and morphology.

### Vessel Staining and Imaging

Eyes were enucleated and fixed in 4% paraformaldehyde for 1 hour. Retinas were then isolated, and the vasculature was stained with 500  $\mu$ L lectin solution (10  $\mu$ g/mL) (Isolectin B4-594; Molecular Probes, Grand Island, NY) overnight and whole mounted flat. Images of the whole retinal mounts were taken at  $\times 5$  magnification using an AxioImager.Z2 microscope (Carl Zeiss, Oberkochen, Germany) with motorized stage. The images were merged using the stitching module in the AxioVision software (Carl Zeiss); to quantify the avascular areas, we used AxioVision software to obtain the total number of pixels in the avascular area and in the entire retina and then calculated the ratio.<sup>16</sup> Neovascularization was analyzed using SWIFT\_NV software to obtain the total number of pixels in the neovascularization area as previously reported.<sup>16</sup> The avascular area and neovascular tufts were established as a percentage of the total retinal area. The determined percentages were then used to compare the injected (PBS or aflibercept) eyes with their noninjected fellow eyes. The results were analyzed by paired *t*-test, determined to best reflect the differences between fellow eyes of a single animal and to control for interanimal variability.

### Hematoxylin-Eosin Staining and Imaging

Eyes were enucleated and fixed in Davidson fixative. They were paraffin embedded and then cut into 5- $\mu$ m sections that were mounted onto slides and stained with hematoxylin-eosin (H&E). Sections were obtained near the optic nerve to obtain full cross-sections of retina (5  $\mu$ m thick) from periphery to periphery. Whole slides were digitized using an  $\times 20$  objective lens and an SL120 Virtual Microscopy Slide Scanner (Olympus; Center Valley, PA). Digital files were analyzed using SlidePath Digital Image Hub and Digital SlideBox software programs (Leica, Buffalo Grove, IL). High-magnification ( $\times 20$ ) images were used to compare the overall structure of the retina, and lower-magnification ( $\times 4$ ) images were used to quantify disruption of the outer plexiform layer (OPL). For quantification, two independent, blinded investigators measured the length of retina without a distinct OPL using a flexible ruler laid directly over the computer images. For each eye, three sections (superior to, through, and inferior to the optic disc) were measured at 5- $\mu$ m widths. Results were reported as a percentage of the entire retinal length. The results were analyzed by paired *t*-test.

### Rhodopsin and Calretinin Immunostaining and Imaging

At P42, three mice from each treatment group were killed. The eyes were enucleated, fixed in Davidson fixative, embedded in paraffin, and cut into 3- $\mu$ m sections. Antigen was retrieved with citrate buffer. The sections were blocked with 0.1 mg/mL AffiniPure Fab Fragment goat anti-mouse IgG (Jackson ImmunoResearch, West Grove, PA) in PBS for 1 hour, washed with PBS, and then blocked again with a solution containing 1% goat serum, 1% BSA, and 0.1% Triton X-100 in PBS. After washing with PBS, they were incubated with primary monoclonal antibody against rhodopsin (1:200 dilution; Millipore, Billerica, MA) for 1 hour at 37°C and subsequently washed with PBS and incubated with secondary antibody conjugated to Alexa 568 (1:500 dilution; Invitrogen, Grand Island, NY). For double immunostaining, sections were washed with PBS and incubated with primary polyclonal antibodies against calretinin (1:200

dilution; Abcam, Cambridge, MA) for 1 hour at 37°C. Calretinin is a neuron-specific calcium-binding protein found mostly in the central nervous system and retina. Studies suggest that calretinin, like calbindin, may be neuroprotective; therefore, alterations in anti-calretinin immunostain may suggest neural injury.<sup>17</sup> After further washing with PBS, they were incubated with secondary antibodies conjugated to Alexa 488 (1:200 dilution; Invitrogen) for 1 hour at room temperature, after which they were rinsed and mounted with Fluoro-Gel mounting medium (EMS, Hatfield, PA).

Images ( $\times 5$  magnification) of the sections were taken when centered on the optic nerve using the AxioImager.Z2 microscope (Carl Zeiss). The retinal width was measured at three locations in each section using the AxioVision software (Carl Zeiss). All measurements were made within 700  $\mu\text{m}$  of the optic nerve. Data were collected from three animals (at P42) from both the high-dose aflibercept and the low-dose aflibercept groups. Additionally, two animals raised in RA were evaluated. The results were analyzed by paired *t*-test.

### Animal Preparation for ERG Analysis

The ERG analysis was completed in the Pediatric Retinal Research Laboratory's retinal imaging and ERG suite of the Eye Research Institute. This workspace is equipped with dim red room lighting (variable 4–15 lux). After 2 hours of dark adaptation, pupils were dilated with sequential application of tropicamide and phenylephrine eyedrops. Short-term anesthesia (30 minutes) was induced by a single injection (intraperitoneal) of 50 mg/kg ketamine hydrochloride and 7 mg/kg xylazine. Corneas were protected by Genteal lubricant solution (Novartis, New York, NY).

### Focal ERG

Focal ERG was used to target the flash stimulus to areas of the retina affected by OIR, which tends to be more central in this model. Focal ERG recordings were collected on dark-adapted mice at P21 ( $\pm 1$  day) and P42 ( $\pm 1$  day) in order to assess retinal function of OIR mice using a Micron III Focal ERG system (Phoenix Research Labs, Pleasanton, CA). Adult mice, raised in RA, were also assessed by focal ERG. Mice were positioned on a regulated temperature pad at 37°C. A gold corneal electrode was integrated into the lens mount of the focal ERG. Platinum cutaneous needle electrodes were used for the reference and ground, inserted into head cap and hind flank skin. Triggering of the LED light stimulus and acquisition of the corneal voltage trace were accomplished with LabScribe-2 software (BioSeb, Vitrolles, France) using the Phoenix Research Labs ERG module. Image-guided aiming of the light stimulus was accomplished by viewing the retina with dim red-filtered LED illumination and high camera gain.

For ERG, an LED white light stimulus was projected on the retina as a circular area. A circular stimulus of 4 disc diameters was centered on the optic disc with an intensity setting of 29 (35,000  $\text{cd}\cdot\text{s}/\text{m}^2$  on the retinal surface) and duration of 30 ms. To compare the injected and noninjected eyes of the same animal, focal ERGs were also collected in four regions immediately adjacent to the optic disc (superior, inferior, nasal, and temporal) using a circular projection of 2 disc diameters. b-Wave amplitudes were averaged from the four locations tested in each eye. Twenty stimulus traces were averaged to generate final ERG traces. b-Wave amplitudes were measured from the minimum of the a-wave to the maximum of the b-wave. Focal ERG was performed on a minimum of four eyes from each group (RA, OIR alone, low-dose aflibercept, and high-dose aflibercept) and time point (P21 and P42). As an additional control, two OIR mice that had PBS injections in

their right eyes were also assessed by focal ERG. Results were analyzed by Student's *t*-test.

## RESULTS

### Avascular Area

Following retinopathy induced by oxygen exposure, subsequent anti-VEGF treatment increased the area of avascular retina at P15 and P17 but recovered by P21 compared with the PBS-injected control and noninjected eyes. There was a near 2-fold increase in the avascular area of aflibercept-treated eyes at P17 compared with the noninjected fellow eyes and PBS-injected eyes (Fig. 1). This trend was dose dependent, with the highest dose of aflibercept resulting in the largest average avascular area. The high dose resulted in a 1.8-fold increase in the avascular area ( $P = 0.001$ ) compared with the noninjected contralateral eye, and the low dose generated a 1.3-fold increase in the avascular area ( $P = 0.023$ ) compared with the noninjected eye. Comparatively, the PBS-treated eyes had a significant decrease (20%) in the avascular area compared with the noninjected fellow eyes ( $P = 0.016$ ), an effect seen previously as well.<sup>18,19</sup> Retinal recovery can occur in response to injury such as that caused by an intravitreal injection. It is feasible that low-grade inflammation following ocular penetration may have a role in retinal recovery.

### Neovascular Changes

Treatment with aflibercept decreased the development of neovascular tufts in the OIR model (Figs. 1A, 2). This effect was seen with both low-dose and high-dose aflibercept regimens (Fig. 2). The high dose caused an 85% reduction in neovascular tufts ( $P = 0.0001$ ), whereas the low dose resulted in a 71% reduction ( $P = 0.0001$ ) compared with the noninjected contralateral eyes. Interestingly, the injection of PBS alone also significantly reduced the neovascular tufts by 48% compared with fellow noninjected eyes ( $P = 0.0001$ ), an effect seen in previous studies<sup>18,19</sup> as well. This could be due to changes in IOP following intravitreal injection or due to increased levels of pigment epithelium-derived growth factor following penetrating ocular injury.<sup>18</sup>

### Retinal Structure

The neurovascular unit<sup>20,21</sup> describes the coordination of angiogenesis with neurogenesis and suggests that delayed retinal vascularization may compromise or alter the development and/or maturation of the neuroretina. Figure 3 shows high-magnification images of H&E-stained cross-sections from eyes of each group at P42. Images were taken in the area adjacent to the optic nerve, correlating with the avascular region seen at an earlier time point (P17). Disruption of the retinal laminar morphology in the oxygen-treated eyes is evident, demonstrating loss of structural architecture of the retinal layers and vacuolization.

In order to quantify the effect of delayed vascular maturation with neuronal changes, the OPL was analyzed in treated (injected) and untreated (fellow noninjected) eyes (Fig. 4). Mature eyes (at P42) were evaluated histologically, specifically looking for disruption of the OPL (Figs. 4A, 4B). Both the low-dose and high-dose aflibercept groups showed increased disruption of the OPL, with a significant disruption in the high-dose aflibercept-treated eyes compared with noninjected fellow eyes ( $P = 0.043$ ). Disruption was seen in the OPL along 36.5% of the retinal length versus only 5.9% in the fellow eyes ( $n = 3$ ). A similar trend was seen in the low-dose group, with an average disruption of 27.9% in injected

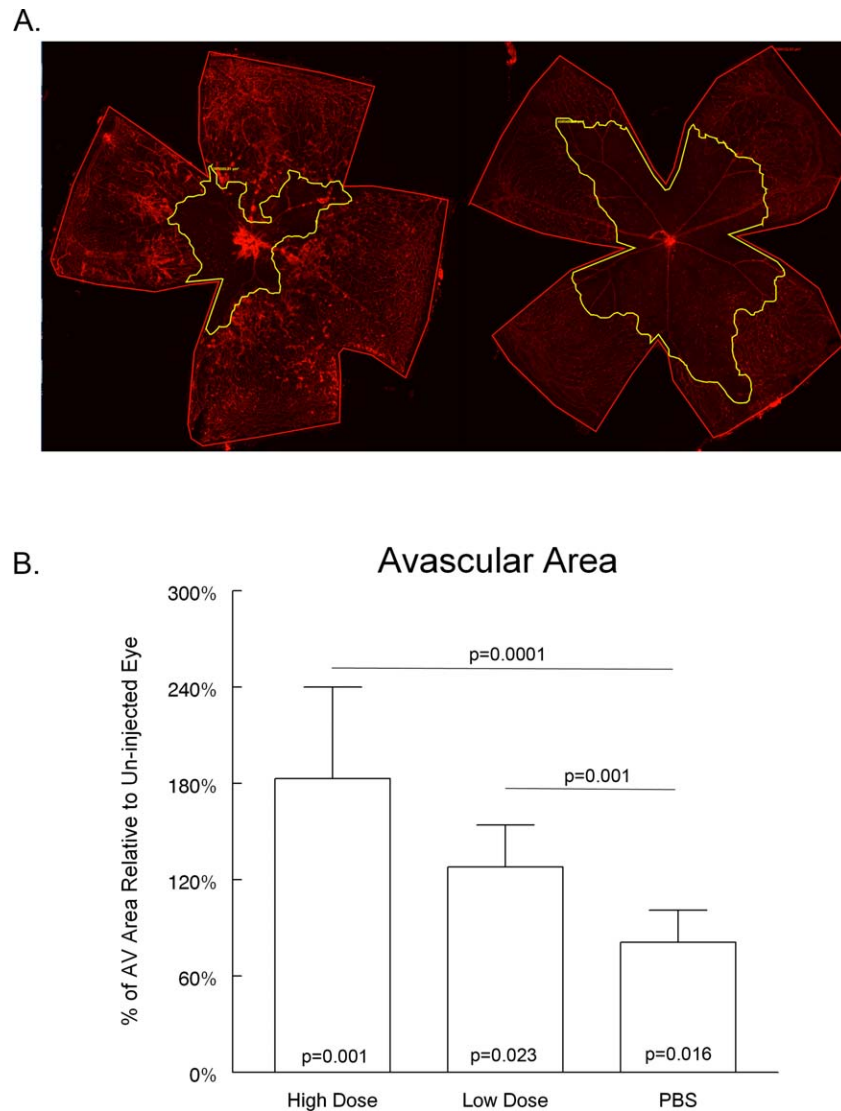


**FIGURE 1.** Aflibercept increases the area of avascular retina at P18 in OIR model mice. **(A)** Images of lectin-stained retinas from OIR mice injected with PBS (*left*) and high-dose aflibercept (*right*). **(B)** A graph depicting the percentage of avascular retina relative to noninjected fellow eyes. The average avascular area is significantly larger in eyes injected with high-dose aflibercept ( $n = 9$ ) and low-dose aflibercept ( $n = 7$ ) compared with noninjected fellow eyes ( $P = 0.001$  and  $P = 0.023$ , respectively). In contrast, PBS-injected eyes ( $n = 9$ ) have smaller avascular areas ( $P = 0.016$ ).

eyes versus 18.6% in fellow eyes ( $n = 3$ ). A smaller, insignificant difference ( $<10\%$ ) was seen in the two PBS-injected eyes compared with noninjected contralateral eyes (Fig. 4C), although considerable disruption was seen in both the injected eye (22.1%) and the noninjected fellow eyes (29.0%). The spectrum of OPL disruption in the noninjected eyes highlights the fact that neural organization in the OIR animal is highly variable. The amount of OPL disruption is consistent within a single test group, however. In order to control for interlitter and interanimal variability as much as possible, each test group consisted of weight-matched littermates. Of note, RA controls did not show any OPL disruption (data not shown).

In more severely affected regions that suffered the most bipolar cell loss, the displacement of mature rod photoreceptor cells and bipolar cells resulted in an incomplete separation of these two cell types. Nocturnal rod photoreceptors have a characteristic chromatin distribution that is unique, with the dense heterochromatin in the nuclear center. This is opposite to most other cells of the body, where the dense heterochromatin is distributed more near the nuclear periphery. This

distribution is visible in H&E-stained sections. Dense rod nuclei were clearly mixed with bipolar neurons, sharing the same depth in some locations.

To further explore disruption of the neural retina caused by oxygen exposure and aflibercept injection, we costained retinal sections with protein markers of rod photoreceptors (rhodopsin) and amacrine cells (calretinin) (Fig. 5A). There was a significant thinning of the retina in the aflibercept-treated eyes compared with the untreated fellow eyes (Fig. 5B). The high-dose eyes had an average retinal thickness of  $140 \mu\text{m}$  (fellow eye,  $166 \mu\text{m}$ ), and the low-dose eyes averaged  $122 \mu\text{m}$  (compared with  $172 \mu\text{m}$  in the untreated fellow eyes). Additionally, disruption of the normal rod photoreceptor cell distribution was seen as intense staining of rhodopsin above the inner/outer segment layers evident in all aflibercept-injected eyes and in a few of the noninjected fellow eyes, but to a lesser extent. Thus, disruption of rod cell distribution was not the result of intraocular injection. Aflibercept-injected OIR eyes appeared to have a reduced number of calretinin-positive (amacrine) cells (Fig. 5A).

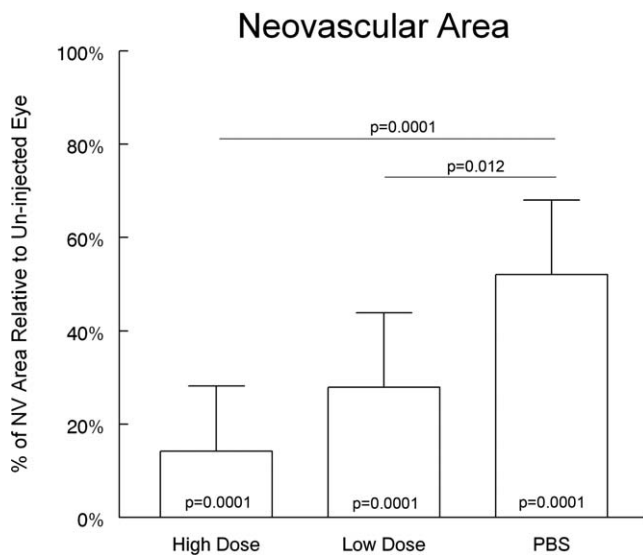


**FIGURE 2.** Aflibercept decreases the amount of neovascularization in P18 OIR mice. The graph depicts the area of retina with neovascularization relative to noninjected fellow eyes. The average area of neovascularization is significantly reduced in eyes injected with high-dose aflibercept ( $n = 9$ ,  $P = 0.0001$ ), low-dose aflibercept ( $n = 7$ ,  $P = 0.0001$ ), and PBS ( $n = 9$ ,  $P = 0.0001$ ).

### Focal ERG

In order to determine the effect of delayed retinal vascularization on retinal function, electrophysiology was performed at two time points using a circular flash stimulus of 4 disc diameters, centered on the disc. The early measurement was taken at P21 (7 days following intravitreal injection) to determine the early effect on function. The untreated OIR

animal eyes ( $n = 13$  at P21 and  $n = 11$  at P42) had a significant loss of function at P21, with some recovery at P42, compared with adult (6 month) RA controls ( $n = 4$ ) (Table, Fig. 6). All b-wave amplitudes were significantly lower in OIR mice (with or without aflibercept) compared with animals that were raised in RA. a-Wave amplitudes were also diminished in OIR mice at both time points, but this trend reached significance in only the low-dose aflibercept group (at P42,  $P = 0.047$ ). Two PBS-injected eyes had a-wave and b-wave amplitudes similar to those of the OIR-alone group (data not shown). Treatment with aflibercept resulted in an even greater loss of function, and this trend reached significance in the low-dose group at P42 ( $P = 0.039$ ) (Fig. 6B). At this later time point, the average b-wave amplitude of the low-dose aflibercept group ( $n = 4$ ) was  $69 \mu\text{V}$  versus  $109 \mu\text{V}$  for the OIR-alone group ( $n = 11$ ). Examples of focal ERGs comparing aflibercept-injected eyes with fellow noninjected eyes are shown in Figure 6C.

Overall, comparison of b-wave amplitudes between the injected (right eye) and noninjected (left eye) eyes of the same animal revealed a relative reduction in b-wave amplitude in the aflibercept-treated eyes. For each eye, b-waves were averaged from the stimulation of four different regions (each 2 disc diameters wide) located adjacent and around the disc. At P21, the mean (SD) ratios of right eyes to left eyes of b-wave amplitudes were less than 1 for the low dose (0.78 [0.20],  $P = 0.05$ ,  $n = 4$ ) and the high dose (0.71 [0.29],  $P = 0.05$ ,  $n = 5$ ). For ERG tests at P42 (different animals from P21 groups), the ratios were not significantly less than 1 for the numbers of animals tested.

### DISCUSSION

Neurogenesis is closely coordinated with angiogenesis in developing tissues.<sup>22</sup> This is of particular interest in the central nervous system tissue because impaired angiogenesis may have

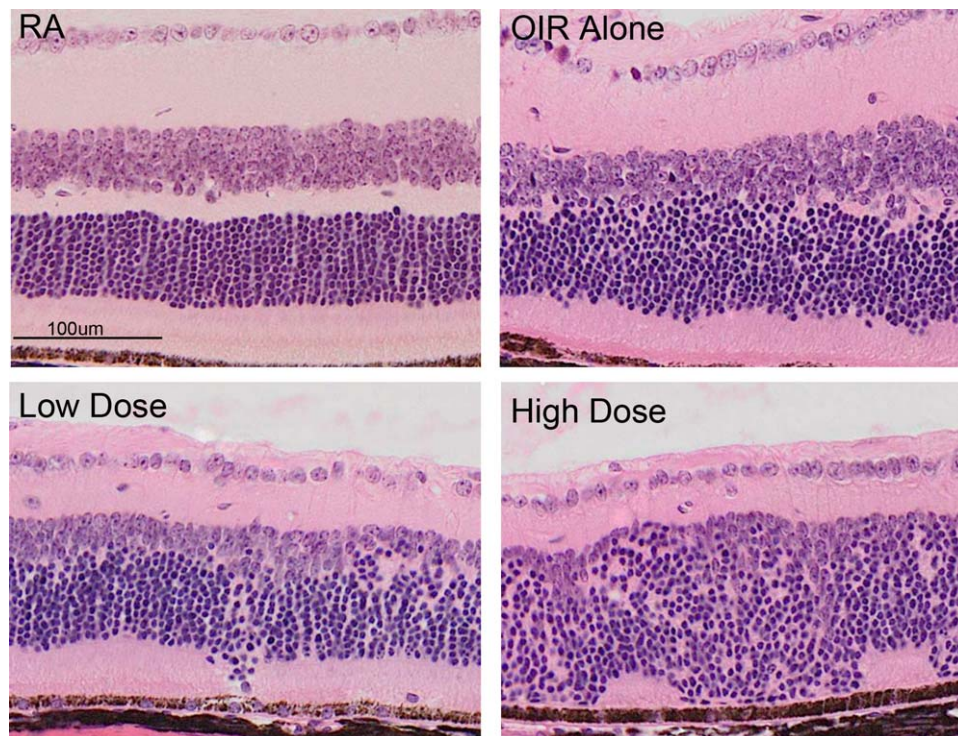


**FIGURE 3.** Disruption of retinal architecture in P42 mice. Shown are representative images of H&E-stained retinal cross-sections. The images were taken adjacent to the optic nerve.

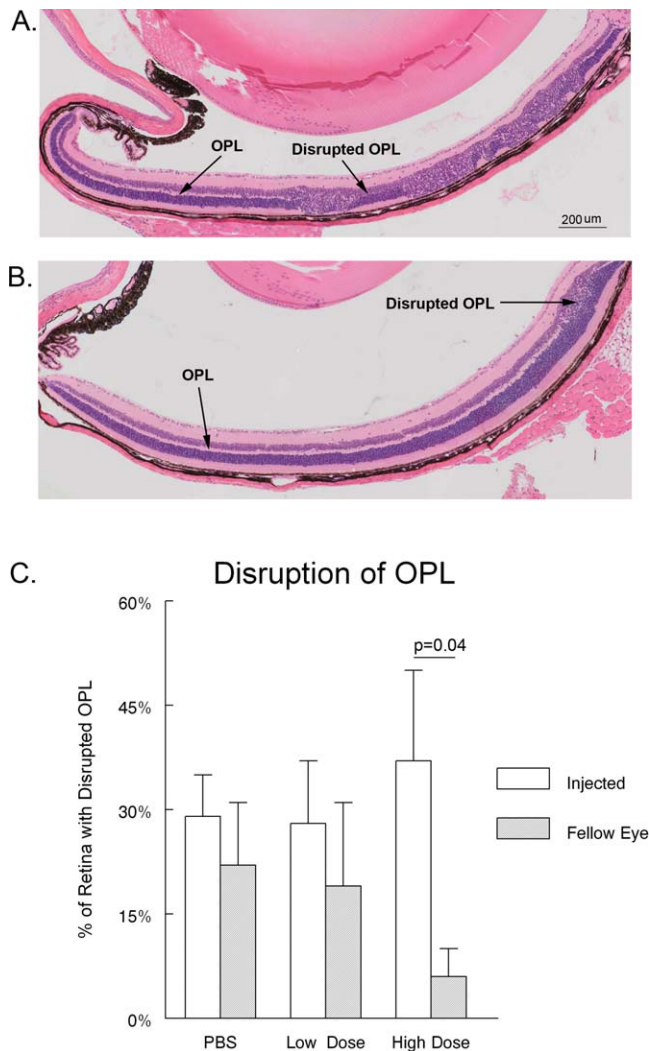


**FIGURE 4.** Disruption of the OPL in OIR eyes. Shown are representative images of H&E-stained retinal cross-sections. (A) High-dose aflibercept-injected eye. (B) Noninjected fellow eye. (C) The graph depicts the percentage of retina with a disrupted OPL. The average percentage is greater in high-dose aflibercept ( $n = 3$ ) and low-dose aflibercept ( $n = 3$ ) eyes versus noninjected fellow eyes.

long-term effects in the neural signaling, maturation, and function of these neurons. The expression of VEGF receptors by vascular and extravascular cells suggests that VEGF modulates both angiogenesis and neurogenesis<sup>25</sup> and that VEGF blockade may directly affect vessel and neuronal growth. Anti-VEGF treatments have been used for the last decade in the treatment of adult retinal vasculopathies due to pathologic overexpression of VEGF. The role of VEGF in neuroprotection and neurogenesis has been an area of investigation in neuroscience, and evidence shows that blockade of VEGF inhibits neurogenesis and causes neurons of the central nervous system to undergo apoptosis.<sup>23</sup> Although the intravitreal anti-VEGF treatments appear to be well tolerated in the adult, their effect on the developing retina has not been extensively studied.

There is increasing use of anti-VEGF treatments in premature infants due to the perceived safety and ease of this treatment option. Our study shows that aflibercept significantly decreases neovascularization in OIR eyes (Fig. 2). Interestingly, PBS injection alone also resulted in a significant decrease in neovascularization. This finding suggests that injection

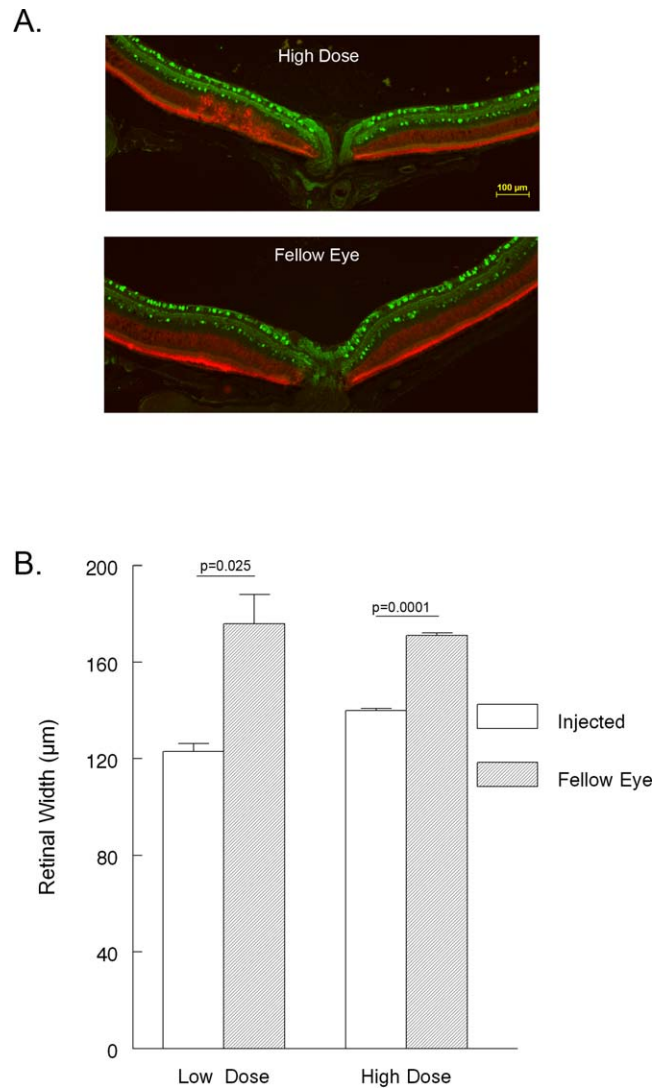


**FIGURE 5.** Disruption of rod photoreceptor and amacrine cells in aflibercept-injected OIR eyes. (A) Rhodopsin-stained (red) and calretinin-stained (green) retinal cross-sections from a high-dose aflibercept-injected OIR mouse. (B) The graph depicts the average width of retina in eyes injected with low-dose aflibercept ( $n = 3$ ) and high-dose aflibercept ( $n = 3$ ) versus fellow noninjected eyes.

alone, perhaps by transient increased IOP, decreases neovascular tufts, a finding previously reported by Tokunaga et al.<sup>19</sup> However, aflibercept has an even greater effect on inhibiting pathologic neovascular growth.

Of growing concern is that anti-VEGF treatment in the context of a developing retina may have unintended consequences. Premature infants, even without the development of retinopathy, demonstrate significant delay in the growth of their retinal vasculature, with maturation often delayed by 12 weeks past their due date. The results of our study show that aflibercept treatment results in a significant increase in the avascular area beyond that caused by the oxygen exposure alone (Fig. 1A). Similarly, in a dog model of ROP, Luty et al.<sup>24</sup> demonstrated slowed revascularization of the retina following intravitreal injection of aflibercept. This finding suggests that the inhibition of VEGF at this stage in development delays the recovery of vascular growth in the retina and exacerbates vascular growth inhibition. Because this animal model closely follows changes seen in ROP, it is likely that delayed vascular

TABLE. Focal ERG a-Wave and b-Wave Amplitudes

Treatment	RA Adult = 137 b-Wave Amplitudes, $\mu\text{V}$		RA Adult = 137 a-Wave Amplitudes, $\mu\text{V}$	
	P21	P42	P21	P42
OIR	82	109	15	17
Low-dose aflibercept/OIR	87	69	12	10
High-dose aflibercept/OIR	59	80	17	14

growth also occurs in premature infants treated with pan-VEGF blockade. An additional concern is the potential effect on neurogenesis in a patient population that already shows functional deficits compared with full-term infants. Mounting evidence suggests that delayed vascular growth retards neurogenesis due to disruption of the normal coordination of neurovascular pathways.<sup>22</sup> In the premature neonate, this may result in incomplete development of the neural retinal tissue.<sup>25</sup>

Although the most obvious way in which VEGF affects the neural retina is by the inhibition of vessel growth, studies<sup>23,26-28</sup> have shown that VEGF itself is directly protective of retinal cells. One study<sup>23</sup> demonstrated a significant decrease

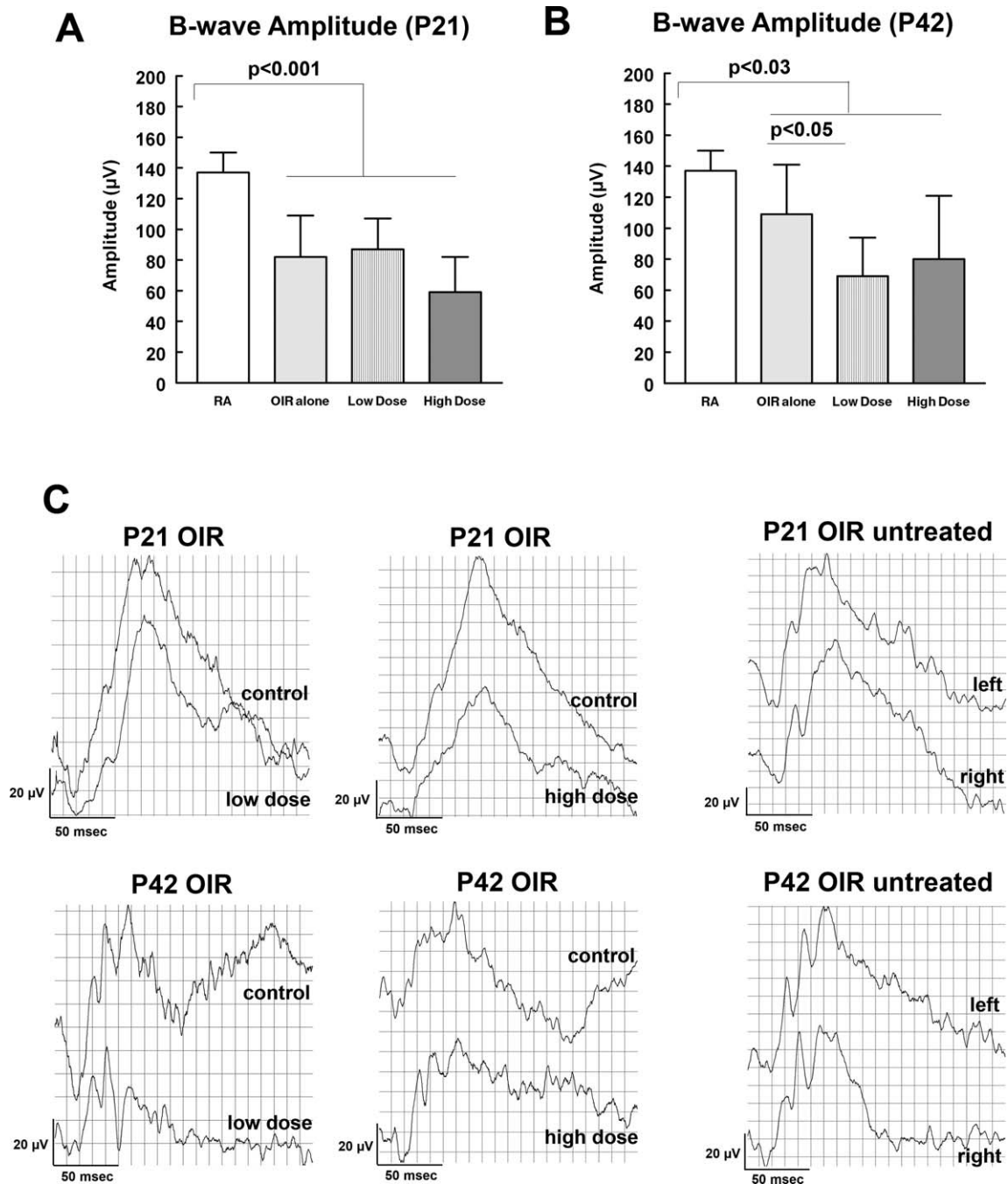


FIGURE 6. Aflibercept further reduces decrease in retinal function caused by OIR. (A, B) The OIR significantly reduces b-wave amplitudes at P21 ( $P \leq 0.001$ ) (A) and P42 ( $P \leq 0.03$ ) (B) compared with adult (6 month) RA mice. Further b-wave reduction was seen in a low-dose aflibercept-injected eye at P42 ( $P = 0.039$ ). (C) Sample focal ERG responses.

in the amount of apoptotic retinal cells with VEGF treatment in a rat model of retinal ischemia. Another study<sup>27</sup> showed Müller, amacrine, and photoreceptor cell death due to VEGF neutralization in adult mice (with no effect upon retinal vessel permeability). Some in vitro investigations also support a role for VEGF-mediated neuroprotection of retinal cells. In one study,<sup>29</sup> VEGF was shown to rescue murine retinal ganglion cells-5 from apoptosis caused by oxidative stress, and this effect was ameliorated by VEGF inhibition with bevacizumab.

Using Ganzfeld (full field) ERG, Nakamura et al.<sup>30</sup> reported a substantial reduction in the OIR b-wave at 4 weeks of age compared with normal mice. Furthermore, they found that the full-field b-wave improved to near normal by 8 weeks of age, although a trend to slightly subnormal values remained. This suggests that focal ERG might be even more useful for analysis of the OIR model because the light stimulation can be limited to the affected central region of the retina.

Full-field ERG stimulates a large portion of undamaged peripheral area, making it difficult to detect local differences in the affected central retina. The focal ERG data presented herein indicate that a delay in vascularization of the retina may have long-term effects on retinal function, even after complete maturation of the retinal vasculature. The function of the neural retina in the original avascular region was still diminished in the eyes of OIR mice and even more so in aflibercept-injected OIR eyes compared with normal mice. It is likely that some bipolar cell loss can be tolerated in the retina as a whole and that the effects on ERG will depend on the severity of bipolar cell loss for an individual mouse and eye.

Using a focal ERG format provides a new method to limit functional testing to smaller retinal zones of more homogeneous morphology. With the smallest focal ERG area used for this study (2 disc diameters), the average b-wave amplitude of four central locations around the disc was less in aflibercept-injected OIR eyes compared with the contralateral noninjected eyes. Morphologic analysis suggests that one possible reason for the reduced b-wave could be a more severe loss of bipolar cells in aflibercept-treated eyes. These focal ERG results also correlate with a general disorganization of the retina's laminar architecture, as well as a significant decrease in retinal thickness in the avascular region of the aflibercept-injected eyes.

These data raise concerns over the use of anti-VEGF treatment in the developing retina, although the inhibition of pathologic vascularization may be of benefit. The question that further investigation must address is the risk-benefit ratio of treating neovascular disease at the expense of inhibiting neurovascular development. Human studies investigating the effect of anti-VEGF treatments on retinal development (both vascular and neuronal) will take years to accumulate and may not be feasible at all. Therefore, extrapolation of data from appropriate animal models may be the best pathway toward understanding the complex biochemical interactions that occur in developing tissues. Continued research will shed light on optimal treatment regimens, but current use of anti-VEGF treatment in the neonate should be approached cautiously.

### Acknowledgments

The authors thank Michael Trese, MD, and Frank Giblin, PhD, for insightful discussion, as well as Oakland University students Keriah Abd and Kristina Mkoyan for assistance during retinal imaging and focal ERG sessions.

Supported by the Vision Research ROPARD Foundation for construction and equipment grants to the Eye Research Institute's Pediatric Retinal Research Laboratory and an operational research grant for pediatric retinal disease models (KPM, KAD).

Disclosure: C.C. Tokunaga, None; K.P. Mitton, None; W. Dailey, None; C. Massoll, None; K. Roumayah, None; E. Guzman, None; N. Tarabishy, None; M. Cheng, None; K.A. Drener, None

### References

- Lafuente JV, Ortuzar N, Bengoetxea H, Bulnes S, Argandoña EG. Vascular endothelial growth factor and other angiogenic factors: key molecules in brain development and restoration. *Int Rev Neurobiol.* 2012;102:317-346.
- Raab S, Plate KH. Different networks, common growth factors: shared growth factors and receptors of the vascular and the nervous system. *Acta Neuropathol.* 2007;113:607-626.
- Siatkowski RM, Dobson V, Quinn GE, Summers CG, Palmer EA, Tung B. Severe visual impairment in children with mild or moderate retinal residua following regressed threshold retinopathy of prematurity. *J AAPOS.* 2007;11:148-152.
- Quinn GE, Dobson V, Davitt BV, et al; Early Treatment for Retinopathy of Prematurity Cooperative Group. Progression of myopia and high myopia in the Early Treatment for Retinopathy of Prematurity study: findings at 4 to 6 years of age. *J AAPOS.* 2013;17:124-128.
- Joyal JS, Sitaras N, Binet F, et al. Ischemic neurons prevent vascular regeneration of neural tissue by secreting semaphorin 3A. *Blood.* 2011;118:6024-6035.
- Smith LE. Pathogenesis of retinopathy of prematurity. *Growth Horm IGF Res.* 2004;14(suppl A):S140-S144.
- Zeng G, Taylor SM, McColm JR, et al. Orientation of endothelial cell division is regulated by VEGF signaling during blood vessel formation. *Blood.* 2007;109:1345-1352.
- Robinson GS, Ju M, Shih SC, et al. Nonvascular role for VEGF: VEGFR-1, 2 activity is critical for neural retinal development. *FASEB J.* 2001;15:1215-1217.
- Schlingemann RO, van Hinsbergh VW. Role of vascular permeability factor/vascular endothelial growth factor in eye disease. *Br J Ophthalmol.* 1997;81:501-512.
- Murakami T, Felinski EA, Antonetti DA. Occludin phosphorylation and ubiquitination regulate tight junction trafficking and vascular endothelial growth factor-induced permeability. *J Biol Chem.* 2009;284:21036-21046.
- Harhaj NS, Felinski EA, Wolpert EB, Sundstrom JM, Gardner TW, Antonetti DA. VEGF activation of protein kinase C stimulates occludin phosphorylation and contributes to endothelial permeability. *Invest Ophthalmol Vis Sci.* 2006;47:5106-5115.
- Cai J, Wu L, Qi X, et al. Placenta growth factor-1 exerts time-dependent stabilization of adherens junctions following VEGF-induced vascular permeability. *PLoS One* [serial online]. 2011;6:e18076. Available at: <http://www.ncbi.nlm.nih.gov/pmc/articles/PMC3064593>. Accessed February 12, 2014.
- Malik S, Vinukonda G, Vose LR, et al. Neurogenesis continues in the third trimester of pregnancy and is suppressed by premature birth. *J Neurosci.* 2013;33:411-423.
- Smith LE, Wesolowski E, McLellan A, et al. Oxygen-induced retinopathy in the mouse. *Invest Ophthalmol Vis Sci.* 1994;35:101-111.
- Stahl A, Chen J, Sapieha P, et al. Postnatal weight gain modifies severity and functional outcome of oxygen-induced proliferative retinopathy. *Am J Pathol.* 2010;187:2715-2723.
- Connor KM, Krah NM, Dennison RJ, et al. Quantification of oxygen-induced retinopathy in the mouse: a model of vessel loss, vessel regrowth and pathological angiogenesis. *Nat Protoc.* 2009;4:1565-1573.
- Lukas W, Jones KA. Cortical neurons containing calretinin are selectively resistant to calcium overload and excitotoxicity in vitro. *Neuroscience.* 1994;61:307-316.

18. Penn JS, McCollum GW, Barnett JM, Werdich XQ, Koepke KA, Rajaratnam VS. Angiostatic effect of penetrating ocular injury: role of pigment epithelium-derived factor. *Invest Ophthalmol Vis Sci.* 2006;47:405-414.
19. Tokunaga CC, Chen YH, Dailey W, Cheng M, Drener KA. Retinal vascular rescue of oxygen-induced retinopathy in mice by norrin. *Invest Ophthalmol Vis Sci.* 2013;54:222-229.
20. Ward NL, Lamanna JC. The neurovascular unit and its growth factors: coordinated response in the vascular and nervous systems. *Neurol Res.* 2004;26:870-883.
21. Carmeliet P, Tessier-Lavigne M. Common mechanisms of nerve and blood vessel wiring. *Nature.* 2005;436:193-200.
22. Bautch VL, James JM. Neurovascular development: the beginning of a beautiful friendship. *Cell Adh Migr.* 2009;3:199-204.
23. Nishijima K, Ng YS, Zhong L, et al. Vascular endothelial growth factor-A is a survival factor for retinal neurons and a critical neuroprotectant during the adaptive response to ischemic injury. *Am J Pathol.* 2007;181:53-67.
24. Luty GA, McLeod DS, Bhutto I, Wiegand SJ. Effect of VEGF trap on normal retinal vascular development and oxygen-induced retinopathy in the dog. *Invest Ophthalmol Vis Sci.* 2011;52:4039-4047.
25. James JM, Gewolb C, Bautch VL. Neurovascular development uses VEGF-A signaling to regulate blood vessel ingression into the neural tube. *Development.* 2009;136:833-841.
26. Foxton RH, Finkelstein A, Vijay S, et al. VEGF-A is necessary and sufficient for retinal neuroprotection in models of experimental glaucoma. *Am J Pathol.* 2013;182:1379-1390.
27. Saint-Geniez M, Maharaj AS, Walshe TE, et al. Endogenous VEGF is required for visual function: evidence for a survival role on Müller cells and photoreceptors. *PLoS One* [serial online]. 2008;3:e3554. Available at: <http://www.ncbi.nlm.nih.gov/pmc/articles/PMC2571983>. Accessed February 12, 2014.
28. Jin KL, Mao XO, Greenberg DA. Vascular endothelial growth factor: direct neuroprotective effect in in vitro ischemia. *Proc Natl Acad Sci U S A.* 2000;97:10242-10247.
29. Brar VS, Sharma RK, Murthy RK, Chalam KV. Bevacizumab neutralizes the protective effect of vascular endothelial growth factor on retinal ganglion cells. *Mol Vis.* 2010;16:1848-1853.
30. Nakamura S, Imai S, Ogishima H, Tsuruma K, Shimazawa M, Hara H. Morphological and functional changes in the retina after chronic oxygen-induced retinopathy. *PLoS One* [serial online]. 2012;7:e32167. Available at: <http://www.ncbi.nlm.nih.gov/pmc/articles/PMC3279421>. Accessed February 12, 2014.